14th INTERNATIONAL WORKSHOP ON RARE EARTH MAGNETS AND THEIR APPLICATIONS, SP (1996) p. 264 - 269
SEPT. 5-9

A COMPARISON OF THE ELECTROCHEMICAL BEHAVIOUR OF Pr-Fe-B AND Nd-Fe-B MAGNETS

I. COSTA, I. J. SAYEG and R. N. FARIA
Instituto de Pesquisas Energéticas e Nucleares - IPEN - CNEN
Caixa Postal 11049 - CEP 05422 -970 - São Paulo - SP

ABSTRACT

In the present work the electrochemical behaviour of Pr-Fe-B sintered permanent magnets has been studied and compared to that of Nd-Fe-B magnets by means of potentiodynamic polarization curves in 0.15 M NaH_2PO_4 deaerated solution. A passive film was formed on the magnets during anodic polarization. Successive polarization cycles resulted in increasingly reduction in the passive current density indicating film growth. The results also suggested that passivation characteristics were slightly better for the Pr-Fe-B magnet than for the commercial Nd-Fe-B magnets investigated.

1. Introduction

Permanent magnets based on Rare Earth-Iron-Boron (RE-Fe-B) have been developed in the last decades[1]. Among the alloys used for producing these magnets, the ternary Nd-Fe-B types are well known due to their excellent magnetic properties. However, they are unstable at medium temperatures and show low aqueous corrosion resistance[2]. This has been attributed to the presence of multiple phases in their microstructure and the large electrochemical potential differences among them[3].

Recently, great interest has been dedicated to Pr-Fe-B magnets, since they present a magnetocrystalline anisotropic field (H_A) higher than that corresponding to Nd-Fe-B magnets, indicating a probable higher intrinsic coercivity ($_iH_c$) associated to the former magnets. Faria et al.[4-7] have published on the high coercivity of sintered Pr-Fe-B magnets produced by the hydrogen decrepitation process.

A few papers have been published on the corrosion/oxidation behaviour of Nd-Fe-B alloys[1,2,8-14]. The literature concerning the corrosion properties of Pr-Fe-B alloys, yet is very scarce[15]. However, it is known that the microstructure of both alloys is complex, and this has naturally a direct consequence on the corrosion properties of these materials.

The microstructure of $Nd_{16}Fe_{76}B_8$ alloys consists of three phases which have been identified as $Nd_2Fe_{14}B$ (matrix phase), $NdFe_4B_4$ (boron rich phase) and the Nd rich phase[11,14]. The electrochemical potential difference among these three phases is significant. Consequently, this alloy is susceptible to galvanic corrosion. According to the literature, the susceptibility to dissolution increases in the following order: $Nd_2Fe_{14}B$, Nd rich phase, and $NdFe_4B_4$ [16]. The potential difference between the main magnetic phase and the Nd rich phase has been reported as around 650 mV, the last phase being more active[17]. Since the main magnetic phase is surrounded by the less noble phases, intergranular corrosion has been reported, and this seems to start on the boron rich phase[16]. Both types of corrosion, galvanic and intergranular appears to occur alongside.

In the present work the electrochemical corrosion behaviour of Pr-Fe-B has been investigated in an acid environment and corresponding commercial Nd-based sintered magnets (STD) were also studied for a comparison.

2. Experimental

Two commercial Nd-Fe-B magnets and a Pr-Fe-B magnet were investigated. The Nd-Fe-B magnets were provided by two different producers and both have composition corresponding to Neomax. These will be named in this paper as STD 1 and STD 2. The $Pr_{16}Fe_{76}B_8$ magnet was laboratory made by powder metallurgy[18]. The materials studied and processing condition are showed in Table 1.

Table 1 - Materials studied and their processing techniques

Material	Processing techniques
STD 1	powder metallurgy
STD 2	powder metallurgy
$Pr_{16}Fe_{76}B_8$	hydrogen decrepitation (HD)

2.1. Surface preparation

After have been cold mounted in an epoxy resin, the surface of the various specimens were prepared by grinding with silicon carbide paper up to grade 1000. The specimens were then degreased with acetone in an ultrasonic bath, rinsed in deionized water, dried in a desiccator over silica gel under vacuum, and then immediately immersed in the test solution.

2.2. Test solution

The test solution used consisted of deaerated 0.15M NaH_2PO_4. The solution was deaerated for at least 1 hour before the test was carried out. The pH of the bulk solution was approximately 4.3. All experiments were conducted at ambient temperature, and the volume of the test solution was approximately 700 ml for each cell. The electrochemical corrosion behaviour was monitored by potentiodynamic polarization curves.

2.3. Experimental set-up

A three electrode set-up was used for performing the potentiodynamic polarization measurements. The experimental cell consisted of working electrode, a saturated calomel reference electrode (SCE), and a graphite counter electrode. Potentiodynamic polarization measurements were carried out by sweeping the electrode potential in the range from the open circuit potential (OCP) to 0.57 V (vs. SCE) and then returning to OCP. Three cycles were performed. The electrode potential sweeping rate was 1 mV/s.

3. Results and Discussion

The potentiodynamic polarization curves for the STD 1 specimens in deaerated 0.15 M NaH_2PO_4 solution are shown in Figure 1.

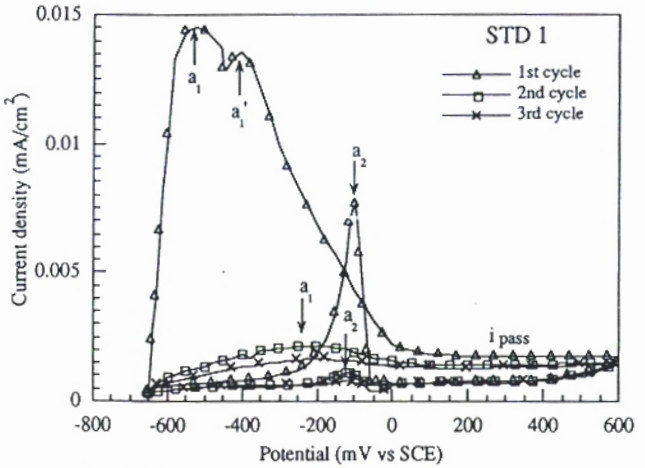

Figure 1 - Polarization curves for STD 1 magnet in deaerated 0.15M NaH_2PO_4 showing three consecutive cycles

It can be seen that an active-passive transition occurs at potentials between -0.55 and -0.40 V (SCE) but the passive film stabilizes at potentials of approximately 0 V (SCE). The current density for passivity, (i_{ccd}), also named a_1 in this paper, was about 15 μA/cm² and the current density in the passive region (i_{pass}) was approximately 2 μA/cm². Two anodic peaks close to each other (a_1 e a_1') were produced during the anodic sweeping and these are shown in figure 1. This indicates that although passivation has started at lower potentials, the film on formation showed a slight dissolution. The passive film formation however prevailed at potentials around -0.40 V (SCE). An anodic peak (a_2) was also shown in the cathodic sweeping direction, at potentials of approximately -0.10 V (SCE), reaching current densities of around 8 μA/cm². The current density decreased again at potentials of approximately -0.20 V (SCE), suggesting that the passive film was unstable at potentials in the range from -0.10 to -0.20 V (SCE). The a_2 peak decreased remarkably after the first cycle and it almost disappeared at the third cycle, indicating the growth of the passive film after each cycle. This was also supported by a progressive drop in current density. The values of a_1 and i_{pass} also decreased after each cycle supporting the film growth supposition.

Figure 2 shows the potentiodynamic polarization curves corresponding to STD 2 magnets. Some common features to STD 1 specimens can be seen in this figure. An active-passive transition is observed to start at potentials around -0.55 V and the film seemed to stabilize at around 0 V. An anodic peak during the cathodic sweeping direction (a_2) was also seen at potentials of approximately -0.10 V and the current density dropped to very low values around -0.20 V. A progressive decrease in current density values was noticed for the second and third polarization cycles which also indicated film growth. The differences found were mainly in the values of i_{pass} and peaks (a_1 and a_2) intensities. The values of a_1, i_{pass} and a_2 for STD 2 specimens were about 60 μA/cm² , 15 μA/cm², and 45 μA/cm², respectively. These are much larger values compared to that produced by STD 1 specimens. Based on these results, it can be said that the STD 2 magnet was more difficult to passivate and the passive film formed on it was less protective as compared to STD 1 magnet.

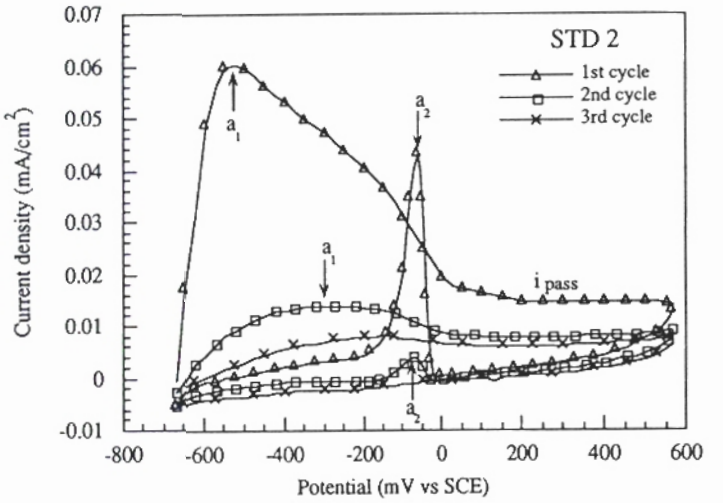

Figure 2 - Polarization curves for STD 2 magnet in deaerated 0.15M NaH_2PO_4 showing three consecutive cycles

The polarization curves produced by $Pr_{16}Fe_{76}B_8$ specimens are shown in figure 3.

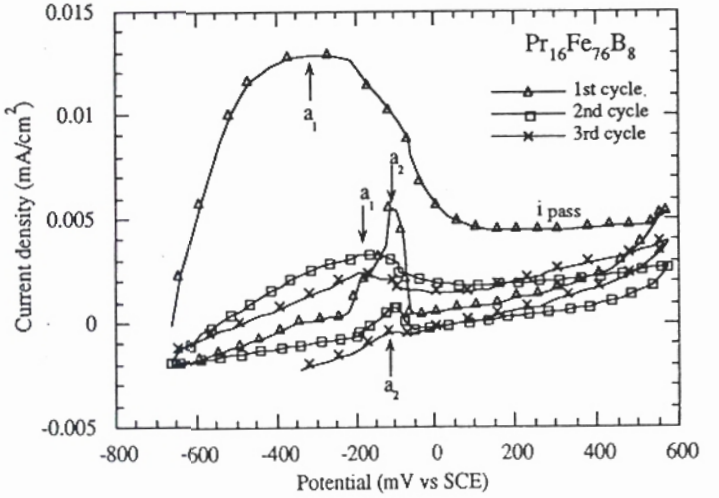

Figure 3 - Three consecutive polarization cycles for $Pr_{16}Fe_{76}B_8$ magnet in deaerated 0.15M NaH_2PO_4 solution.

The $Pr_{16}Fe_{76}B_8$ specimens also showed an active region followed by an active-passive transition. The potential at which the passive film stabilized was the same as for the other magnets studied, 0 V (SCE). For $Pr_{16}Fe_{76}B_8$ specimens, a_1, i_{pass} and a_2 were approximately 13 $\mu A/cm^2$, 4 $\mu A/cm^2$, and 5 $\mu A/cm^2$, respectively, indicating that passivation was easier for this magnet when compared to the other ones studied. The passive film on this magnet presented protective characteristics similar to that formed on STD 1 magnets, although slightly larger passive current densities were produced by $Pr_{16}Fe_{76}B_8$. The peak a_2 decreased progressively after the first cycle, also implying that the film on the alloy grows thicker after each cycle.

The first cycles of the three magnets studied were overploted for comparison reasons, and these are shown in figure 4. It can be noticed that the passivation characteristics were common for all the alloys investigated. However, STD 2 specimens presented much larger current densities and were also more difficult to passivate as compared to the other alloys. The film formed was also less protective on STD 2 specimens . It can also be noted that current density values for STD 1 and $Pr_{16}Fe_{76}B_8$ specimens, were very close at most polarization potentials. Nevertheless, from the results produced the three magnets investigated could be ranked in the following order, according to the difficult in reaching passivity; STD 2 > STD 1 > $Pr_{16}Fe_{76}B_8$.

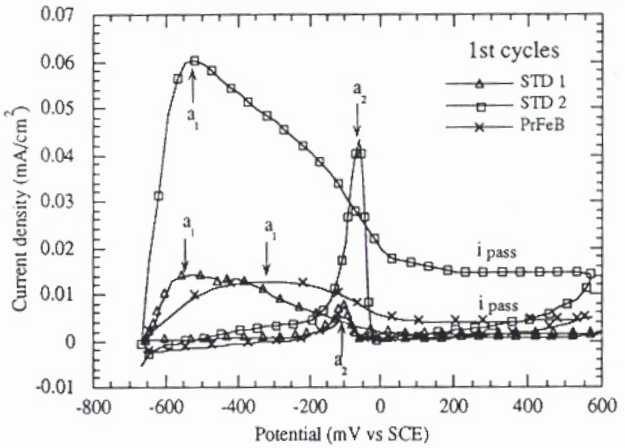

Figure 4 - First potentiodynamic polarization cycles of $Pr_{16}Fe_{76}B_8$, STD 1, and STD 2 magnets in 0.15 M NaH_2PO_4 deaerated solution

4. Conclusions

(1) Active-passive transition was observed for all the magnets used in this investigation.

(2) The passive film was stable at potentials greater than 0 V (SCE), however it showed dissolution between -0.10 and -0.20 V (SCE) at the reverse scan (cathodic direction).

(3) Successive polarization cycles caused passive film growth indicated by the increasingly reduction in a_2 peak height and in current density.

(4) Passivation was slightly easier for $Pr_{16}Fe_{76}B_8$ as compared to STD1 specimens studied.

(5) The passivation characteristics of the STD2 used were however much inferior to that corresponding to the other alloys investigated.

5. Acknowledgements

Acknowledgements are due to Sumitomo Special Special Metals Co. and Crucible Magnetics for the provision of the magnets. Thanks are due to Rare Earth Products for the provision of the Pr alloys. The authors express their thanks to Alloy Chemistry group of the University of Birmingham for the provision of research facilities. Gratitude is also due to CNPq, FAPESP and IPEN/CNEN for financial support granted for the realization of this work.

6. References

1. M. Sagawa, S. Fujimura, N. Togawa, H. Yamamoto and Y. Matsuura, *J. Appl. Phys.* **55** (6), 1984, 2088.
2. E.D. Dickens Jr., and A.M. Mazany, *J. Appl. Phys.* **67** (9), 1990, 4613-4615.
3. G.W. Warren, G.Gao and Q. Li, *J. Appl. Phys.* **70** (10), 1991, 6609-6611.
4. R. N. Faria, J. S. Abell and I. R. Harris, *J. Appl. Phys.* **70** (10), 1991, 6104.
5. R. N. Faria, J. S. Abell and I. R. Harris, *Journal of Alloys and Compounds* **185** 1992, 81.
6. X. J. Yin, M. G. Hall, I. P. Jones, R. N. Faria and I.R. Harris, *J. Magn. Magn. Mater* **125**, (1993), 78.
7. R. N. Faria, X. J. Yin, J. S. Abell and I. R. Harris, *J. Magn. Mater.* **129** (1994) 263.
8. S.Hirosawa, S Mino, and H. Tomizawa, *J. Appl. Phys.* **69** (8), 1991, 5844-5846.
9. C.J. Willman and K.S.V. L. Narasimhan, *J. Appl. Phys.* **61** (8), 1987, 3766-3768.
10. K. Tokuhara abd S. Hirosawa, *J. Appl. Phys.* **69** (8), 1991, 5521-5523.
11. H. Bala, G. Palowska, S. Szymura, V.V. Sergeev and Y.M Rabinovich, *J. Magn. Mater.* **87**, (1990), 1255-1259.
12. A.S. Kim, F.E. Camp, and E. J. Dulis, *IEEE Trans. Magn.* **26** (5), 1990, 1936-1938.
13. P. Tenaud, F. Vial and M. Sagawa, *IEEE Trans. Magn.* **26** (5), 1990, 1930-1932.
14. J. Jacobson and A. Kim, *J. Appl. Phys.* **61** (8), 1987, 3763-3765.
15. H.H.Stadelmaier, N.A.Elmasry, N.C.Liu, and S. Cheng, *Mater. Lett.* **2**, 184, 414.
16. T. Minawo, M. N. Yoshikawa and M. Honshima, *IEEE Trans. Magn.* **25** (5), 1989, 3776-3778.
17. W. Bloch, K. Grendel e H. Staubach, in *Proceedings Eleventh International Workshop on Rare Earth Magnets and Their Applications*, Pittsburgh, Pa, 21-24 October 1990, 108-122.
18. R.N. Faria, A.J. Willliams, J.S. Abell and I.R. Harris, this conference